Numerical Analysis of the Shapes and Energies of Droplets on Micropatterned Substrates

Dominique Chatain,*,[†] Dan Lewis,[‡] Jean-Pierre Baland,[§] and W. Craig Carter[||]

Centre de Recherche en Matière Condensée et Nanosciences, Laboratoire Propre du CNRS associé aux Universités d'Aix-Marseille 2 et 3, CNRS, campus de Luminy, case 913, 13288 Marseille Cedex 9, France, Ceramic and Metallurgy Technologies, General Electric Company, Building MB-223, One Research Circle, Niskayuna, New York 12309, Centre de Recherche de Modélisation Moléculaire, Université de Mons-Hainaut, Parc Initialis, Avenue Copernic, 7000 Mons, Belgium, and Department of Materials Science and Engineering, Massachusetts Institute of Technology, Cambridge, Massachusetts 02139

The shapes and energies of drops on substrates patterned with either holes or posts are computed using Surface Evolver software. The holes and posts are cylindrical in shape and distributed in a 6-fold symmetric pattern. The wetting conditions are such that the liquid does not fill the holes and the interface between the drop and the substrate is composite, i.e., partly solid/liquid and partly liquid/vapor. The sequence of stable drop configurations with increasing volume is analyzed and provides, in part, an explanation for superhydrophobic drop spreading.

Introduction

Wetting and spreading of a drop on a heterogeneous surface is related to the pinning of its triple line. When a solid surface is two-phased, made up of discontinuous patches of one phase on another, and the equilibrium (or Young) contact angles of a liquid on these two phases are larger than few degrees, the motion of the triple line across the field of discontinuous surface features cannot be analytically solved. This paper focuses on surfaces where composite wetting takes place, i.e., for drops with macroscopic contact angles much larger than 90°. This surface phenomenon was identified in 1964 by Dettré and Johnson[1] during studies of wetting of water on rough wax surfaces. It also takes place when metallic liquids are in contact with inert rough oxide surfaces.[2] In the framework of wetting by water, the composite wetting phenomenon has recently been renamed superhydrophobicity and is a topic which has received a great deal of recent interest. To explain some of the experimental features described in the companion paper,[3] Surface Evolver software is used here to calculate the shape and energy of drops on surfaces with cylindrical holes and posts distributed in a 6-fold symmetric pattern. That software was also used recently to investigate the shape of drops on a rough surface.[4] This computational approach can provide a means for optimizing the superhydrophobicity of surfaces.

Evolver Data File for Composite Interfaces

Surface Evolver[5] is an interactive, finite-element-based program for the study of surface-energy-defined shapes. Given a set of user-defined surfaces and constraints, the program adjusts the geometric elements of the surface toward a minimum energy configuration using a conjugate gradient method. Because it minimizes total energy (which may include a combination of surface and gravitational energies) and can handle arbitrary topology as well as a wide range of constraints (such as constant volume and contact angle), Surface Evolver is well suited to modeling the shape of drops on two-phase surfaces.

In this paper, the shapes of drops are calculated in the absence of gravity. The drop resides on a two-phase surface that consists of a continuous so-called "matrix" (phase 1), containing discontinuous circular patches (phase 2). Two cases are considered: one where the patches are holes and the matrix is solid and a second where the patches are solid and the matrix is a hole. In both cases, the circular patches occupy 50% of the substrate surface area and the distance between their centers is 1 unit of length. All of the linear dimensions are expressed in terms of this unit. The interface where the liquid does not contact the solid, i.e., above the holes, is defined to be flat and coplanar with the solid/liquid interface. This assumption is not strictly true as the liquid surface curvature should be constant at any point of the surface (in the absence of gravity) as noted by the Laplace equation. In the absence of gravity, this equation can be written as

$$\Delta P = \gamma_{LV} \left(1/R_1 + 1/R_2\right) \tag{1}$$

where ΔP is the constant difference in pressure across the liquid surface, γ_{LV} is the surface energy of the liquid, and R_1 and R_2 are the two principal radii of curvature of the surface.

If one of the in-plane dimensions of the hole is small relative to the size of the drop, the liquid surface above the hole is nearly flat.[6]

The interfacial potential energy part of the total configurational energy of a drop calculated with Evolver is

$$E = \gamma_{LV}A_{LV} + \Sigma(\gamma_{SL} - \gamma_{SV})A_{SL} \tag{2}$$

where γ_{IJ} are the energies of the interfaces IJ (liquid/vapor, solid/vapor, and solid/liquid) and A_{IJ} are the areas of the interfaces.

* Corresponding author.
[†] CNRS.
[‡] General Electric Company.
[§] Université de Mons-Hainaut.
[||] Massachusetts Institute of Technology.
(1) Dettré, R. H.; Johnson Jr., R. E. *Adv. Chem. Ser.* **1964**, *43*, 136.
(2) De Jonghe, V.; Chatain, D.; Rivollet, I.; Eustathopoulos, N. *J. Chim. Phys. Fr.* **1990**, *87*, 1623.
(3) Chatain, D.; Lesueur, C.; Baland, J. P. *Langmuir* **2006**, *22*, 4230.
(4) Patankar, N. A.; Chen Y. *Proceedings of the 5th International Conference on Modeling and Simulation of Microsystems* San Juan, Puerto Rico, 2002.
(5) Brakke, K. A., 2003, The Surface Evolver, http://www.susqu.edu/facstaff/b/brakke/evolver.
(6) Bico, J.; Marzolin, C.; Quéré, D. *Europhys. Lett.* **1999**, *47* (2), 220.
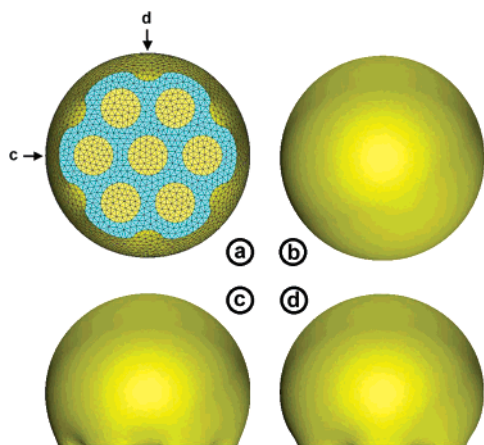
Figure 1. Different views of a drop sitting on seven holes. (a) The bottom view displays the wandering of the triple line; (b) top view; (c) side view corresponding to the largest contact diameter (horizontal arrow in panel a); (d) side view corresponding to the smallest contact diameter (vertical arrow in panel a).

The summation in eq 2 pertains to the interface between the drop and the substrate and accounts for the heterogeneity of the interface that is made up of hole and planar solid. For each of these components of the substrate, an equilibrium contact angle can be defined as follows:

$$(\gamma_{SL} - \gamma_{SV}) = -\gamma_{LV} \cos \theta_E \tag{3}$$

Thus, E may be written

$$E = \gamma_{LV}[A_{LV} - \Sigma A_{SL} \cos \theta_E] \tag{4}$$

which shows that the energy of the drop scales with the liquid surface energy.

The θ_E values used in the calculations are 110° on the solid surface (which is the contact angle of Pb on SiO_2 found in the companion paper[3]) and 180° on the top of a hole. For the sake of simplicity, the liquid surface energy has been set to a value of 1 unit of surface energy.

Example of Shape

Figure 1 shows four views of a calculated drop residing over 7 holes in the substrate. The volume of the drop is 23 (length unit)[3], and the stability of the drop at this volume and in this configuration has been verified. That is, any small deviations from the drop shape and position displayed in Figure 1 are unstable.

The top left image (Figure 1a) is a view from the bottom of the drop and shows the solid/liquid interface (in blue) and the coplanar liquid surface above the circular holes (in yellow). This image shows the discretization of the surfaces and interfaces into triangular areas as performed by the Evolver software. The triple line of the drop wanders around a mean circular position: it is indented along the edges of the next ring of holes and protrudes on the planar solid surface between them. The local contact angle varies along the triple line: on the plain solid surface, it approaches the equilibrium contact angle of 110°, and where the triple line touches the edges of the next ring of holes, it ranges between 110° and 180°. The calculated local contact angle in the finite-element simulation will deviate from the true local angle depending on mesh refinement. In the vicinity of the triple line, the surface shape of the drop deviates from a spherical cap because of the wandering of the triple line. The images in panels c and d are two noteworthy profiles of the sessile drop marked by arrows in Figure 1a. In the profile in panel c, the contact diameter

of the drop is a maximum and the local contact angle is equal to 110°, the equilibrium contact angle on the solid surface. The radius of curvature at the top of the drop is R_{t1}. Fitting the drop surface with a circle of radius R_{t1} gives an estimate of 120° for the macroscopic contact angle. Thus, the drop profile protrudes out of that fitted circle in the vicinity of the substrate. In the profile in panel d, the contact diameter is a minimum. The radius of curvature at the top of the drop, R_{t2}, is equal to R_{t1}. The circle of radius R_{t2}, almost fits the whole drop profile. When approaching the junction with the substrate, the liquid surface deviates inward toward the center of the fitted circle, because the triple line is pinned to the edge of the uncovered holes. For both of the profiles in panels c and d, the liquid surface deviation is of the order of the wandering length of the triple line on the pinning defects. The top view of the drop profile in panel b is a circle of radius $R_t = R_{t1} = R_{t2}$. For this drop, the liquid surface deviation in the vicinity the foot of the drop does not extend above the equatorial diameter of the drop. Thus, the macroscopic angle of 120° can be estimated by fitting any drop profile with the Laplace equation, as long as the fitting process is truncated at a distance from the substrate equal to the amplitude of the triple line wandering on the defects.

Energy of a Drop

In the following discussion, we investigate changes in the shape and energy of a drop as a function of volume and number of circular defects contacted at the interface. It is convenient to discuss the relative stabilities of drops of different volumes by comparing their normalized energy, written in the following manner:

$$E_{norm} = E/\gamma_{LV}(V^{2/3}) \tag{5}$$

where V is the volume of the drop.

E_{norm} is a dimensionless number that characterizes the equilibrium state of a drop shape. For identical wetting conditions, this number has a constant value for different volumes of liquid. For example, consider a sessile drop on a smooth surface containing no discontinuities, where E_{norm} is a function of only its equilibrium contact angle, θ_E. Figure 2a shows E_{norm} for the sessile drop as a function of θ_E, which is here equivalent to its macroscopic contact angle. This curve is independent of the volume of the drop; that is, any sessile drop of equilibrium contact angle, θ_E, has the same E_{norm}, given by one point on the curve of Figure 2a.

We can use E_{norm} to discuss the wetting hysteresis of a sessile drop because the location of its triple line depends on its volume. If we fix the triple line of a drop at its equilibrium position for a given volume, E_{norm} becomes dependent on the volume of the drop. Starting with a volume of 1, the normalized energy of such a constrained drop with $\theta_E = 110°$ was calculated as a function of its volume. The result is displayed in Figure 2b. The curve has a minimum at a volume of 1 where the macroscopic angle is equal to θ_E. This minimum corresponds to the stable shape of the drop. For any volume other than 1, the drop shape is constrained and metastable. Assigning the constraint to the triple line, the additional elastic energy due to the nonequilibrium position of the triple line can be written as

$$E_{el} = \frac{1}{2}k_e(x - x_0)^2 \tag{6}$$

where k_e is the elastic constant of the triple line and x and x_0 are the constrained and equilibrium positions of the triple line, respectively.

Figure 2c compares the normalized energies of constrained and free sessile drops (Figure 2a) as a function of their macroscopic
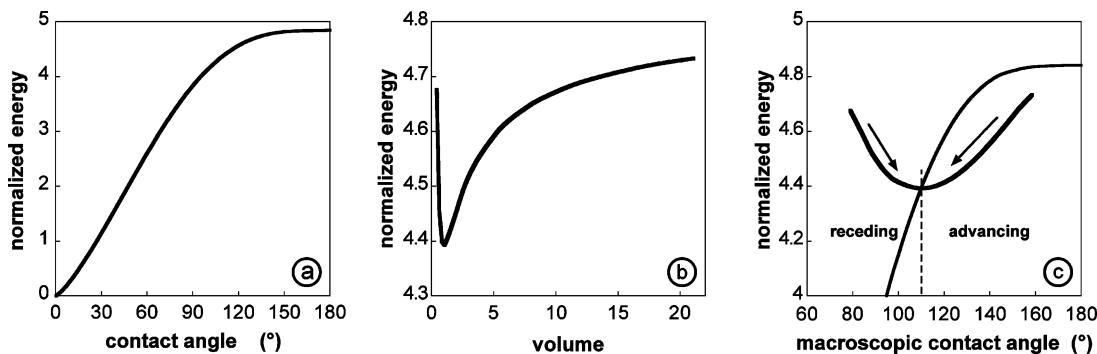
Figure 2. (a) Normalized energy of a free sessile drop as a function of its equilibrium contact angle; (b) normalized energy of a sessile drop of 110° equilibrium contact angle, with a triple line fixed at the equilibrium position corresponding to a volume of 1, as a function of drop volume. (c) Comparison of the normalized energies of a constrained sessile drop with a 110° equilibrium contact angle (black line) and of a free (grey line) sessile drop as a function of their macroscopic contact angles.
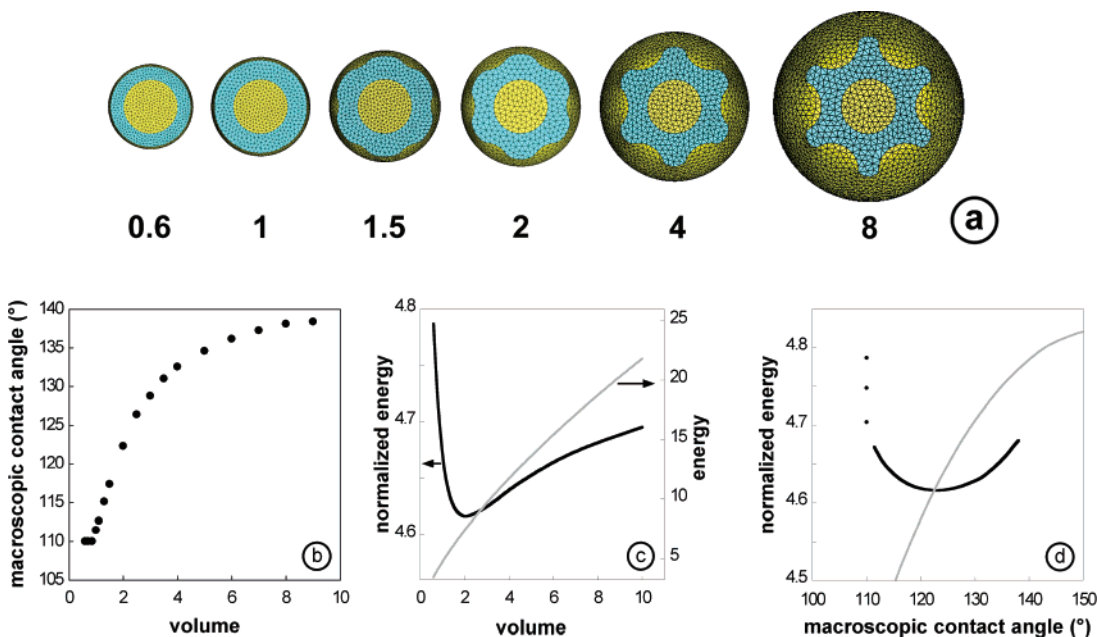
Figure 3. (a) Bottom view of a series of drops of different volumes sitting on one hole. The equilibrium contact angle on the solid is 110°. The volume of each drop is given under each picture. (b) Macroscopic contact angle (calculated from the drop height and the radius of curvature at its top) as a function of the drop volume. (c) Normalized energy (black line) and energy (grey line) of a drop on one hole as a function of volume. (d) Normalized energy of a drop on one hole (black line) and of a free sessile drop (grey line) on a plain solid surface as a function of their macroscopic contact angles.

contact angles. When the constraint on the triple line is released, the drops with macroscopic angles lower or higher than 110° recede or advance, respectively.

Throughout the remainder of this discussion, the normalized energy will be used for discussing the stability of different configurations of a drop residing on different numbers of defects as its volume is increased or decreased.

Shape and Energy of a Drop Centered on 1 and 3 Holes

Figure 3a presents a series of calculated drops centered on-top of 1 hole as viewed from beneath the drop. The volume of each drop is given under each picture. The equilibrium contact angle on the solid is 110°. Figure 3b shows the macroscopic contact angles of these drops as a function of volume. These angles are calculated from the radii of curvature at the top of the drops, R_t, and the heights of the drop, h_t, both computed by Surface Evolver, as follows:

$$\cos(\theta_{macro}) = (1 - h_t/R_t) \tag{7}$$

In Figure 3c, both the total and normalized energies of the drop

are plotted as a function of volume. The total energy increases monotonically with the volume; however, there is a minimum in the normalized energy near a volume of 2. This minimum in normalized energy corresponds to the stable drop shape. For any other volume, the drop shape is metastable. Figure 3d compares the normalized energies of a drop centered on 1 hole and of a free sessile drop (similar to Figure 2a) as a function of their macroscopic contact angles. The stable drop centered on 1 hole has the same normalized energy as a free sessile drop on a plain solid with an equilibrium contact angle of 123°. For that stable drop centered on 1 hole, the area fraction of the solid/liquid interface was found to be 69.8% from the Surface Evolver calculation. For a two-phase surface, the relationship between area fraction and equilibrium contact angle has been described by Cassie and Baxter[7] and is given by

$$\cos \theta_{CB} = a^{solid} \cos \theta_E^{solid} + a^{hole} \cos \theta_E^{hole} \tag{8}$$

where a^i is the area fraction of each component of the interface (solid/liquid or liquid/vapor).

---

(7) Cassie, A. B. D.; Baxter, S. *Trans. Faraday Soc.* **1944**, *40*, 546.
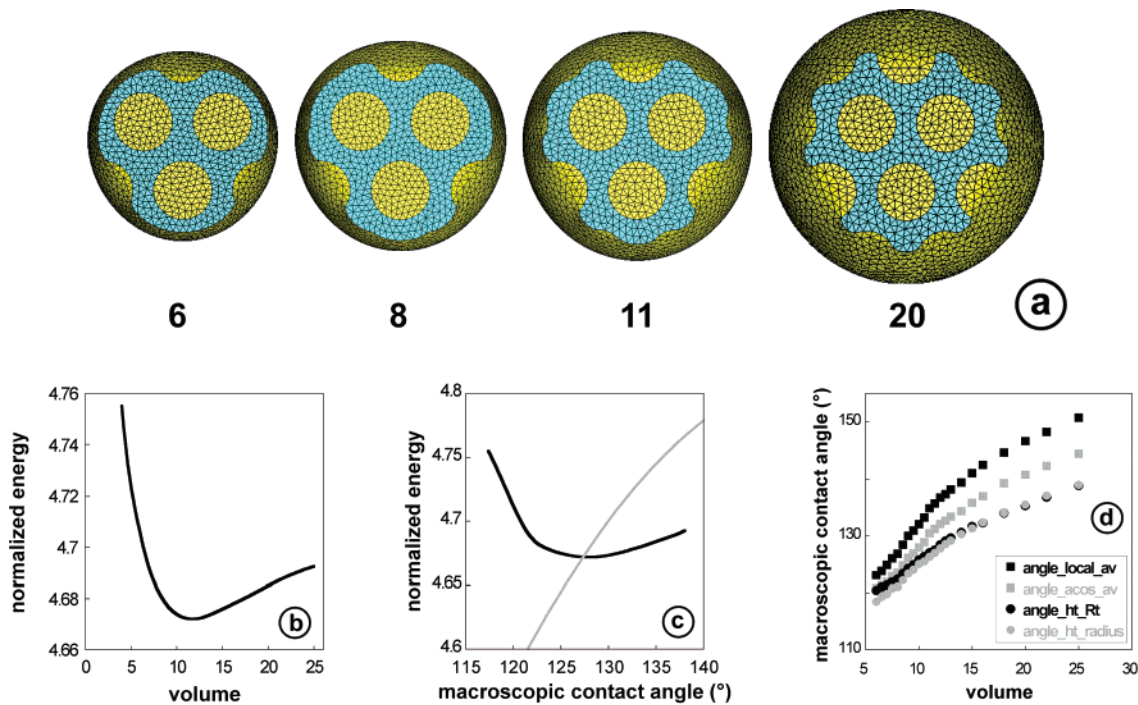
Figure 4. (a) Bottom view of a series of drops of different volumes sitting on top of 3 holes. (b) Normalized energy of a drop on top of 3 holes as a function of its volume. (c) Normalized energy of a drop on top of 3 holes and of a free sessile drop as a function of their macroscopic contact angles. (d) Macroscopic contact angles as a function of the volume of the drop; angle_h_t_R_t is calculated with eq 7; angle_h_t_radius is equal to 2 atan(h_t/r) where r is the average contact radius of the drop. r is the average of the distances between the drop center and the middle of each edge (tl_{local}) along the triple line; angle_local_av is the average of the local contact angles of each triangle of the liquid surface along the triple line ($\theta = \Sigma(tl_{local}\theta_{local})/\Sigma \, tl_{local}$); and angle_acos_av which is equal to acos($\Sigma(tl_{local} \cos \theta_{local})/\Sigma \, tl_{local}$) results from a Cassie type energy average along the triple line.

Using the area fraction calculated by Surface Evolver, the Cassie−Baxter contact angle is found to be 123°. This result is not a coincidence. Indeed, θ_{CB} decreases as the volume of the drop increases due to the increase of the area fraction of the actual solid/liquid interface. Thus, the stable drop centered on 1 hole has the equilibrium angle for that heterogeneous surface. If we refer to the previous discussion of the hysteresis of a sessile drop, the stable drop shape centered on 1 hole has an unconstrained triple line. This shape corresponds to a unique optimization of the areas of the different interfaces of the drop on the solid. Only a numerical minimization such as that enabled by Surface Evolver can handle the complexity of such drop shapes to allow the present analysis.

For a droplet having a constant macroscopic contact angle of 110°, Figure 3c shows that the normalized energy first decreases as the volume of the drop increases. The decrease in energy up to a volume of 1 is related to the increase in the fraction of the solid/liquid interfacial area. This decrease continues until the volume is approximately 2. For drop volumes other than 2, there is an additional elastic energy due to the nonequilibrium position of the triple line.

Figure 4a−d displays data related to drops placed symmetrically over 3 holes. Their wetting behavior is similar to that of drops centered on 1 hole. Figure 4a presents a series of drops centered on 3 holes, viewed from the bottom, as a function of drop volume. At lower volumes, the triple line touches the edges of three neighboring holes, and above a volume of 8, the triple line partly runs along the edges of nine neighboring holes. As the volume increases beyond 8, the equatorial diameter of the drop increases faster than the mean contact diameter. Thus, as for the drop on top of 1 hole, the macroscopic contact angle increases with the volume of the drop.

The normalized energy plotted against drop volume in Figure 4b and against the macroscopic contact angle in Figure 4c displays

the same trends as those observed for a drop on top of 1 hole. For the smallest and the largest volumes investigated, the calculated shapes are metastable. The normalized energy has a minimum for a volume of about 11.5 and a macroscopic contact angle of 127°. Comparison with the normalized energy with a free sessile drop shows again that the minimum corresponds to the stable unconstrained shape of the drop. The area fraction of the actual solid/liquid interface calculated with Evolver is 64.7%. It corresponds to a macroscopic Cassie−Baxter angle of 125°, which is close to the macroscopic contact angle of 127°, calculated for a volume of 11.5. The discrepancy between these two angles is related to the large number of triangles required to calculate a drop with a complex shape. Further refinement of the mesh may improve the correlation; however, this has not yet been attempted.

From the geometric data of the shape of the drop given by Evolver, different macroscopic contact angles can be calculated. These are plotted in Figure 4d as a function of the volume of the drop. The figure caption gives details on the methods of calculation. All of the curves display increasing contact angles with the increasing volume of the drop. The two smallest macroscopic angles are calculated from the macroscopic dimensions of the drop (height, radius of curvature, and average contact radius). They have similar values, consistent with measurements at the macroscopic scale. The two largest angles are determined by using an average of local contact angles along the triple line. These clearly deviate from the measurable macroscopic contact angle. Thus, the local angles do not determine the macroscopic contact angle of a drop.

Comparison between Different Configurations of Drops

Drops on Holes. For a more complete analysis, we have calculated the shape of drops on highly symmetric positions with respect to a distribution of circular holes. We have selected
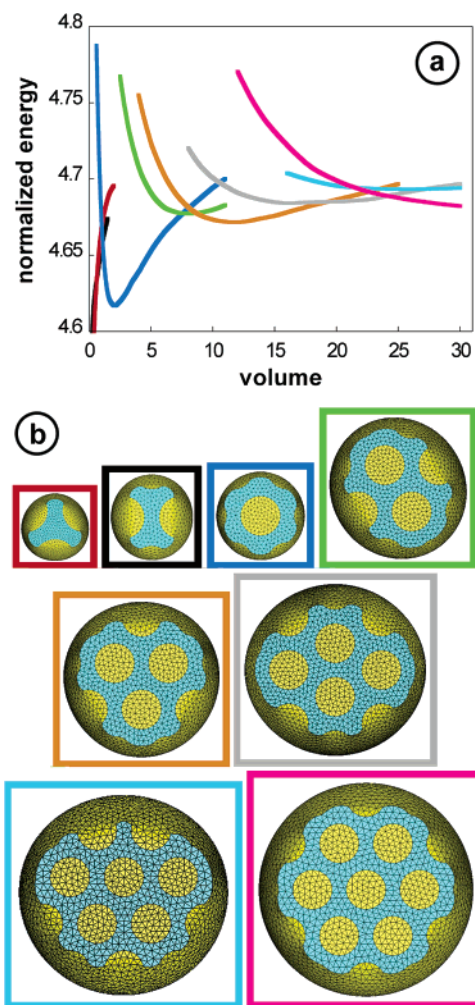
Figure 5. (a) Normalized energy of drops of different configurations on a substrate with holes; (b) the bottom views of the different configurations calculated with Evolver.

drops between 3 holes, between 2 holes, and on top of 1, 2, 3, 4, 5, and 7 holes. The 6-hole configuration was always found to be unstable relative to the 5- and 7-hole configurations. For a given volume, the stability of each configuration was checked by displacing the drop slightly along pertinent paths (generally high-symmetry axes of the pattern) and allowing Evolver to move the drop so as to reach the minimum configuration energy.

Figure 5a shows the normalized energy curves as a function of the drop volume for the different configurations calculated. For each configuration, the normalized energy is calculated for volumes around the minimum value. As discussed previously, the minima in normalized energy correspond to the stable configurations. Bottom views of each of the calculated configurations are shown in Figure 5b. The color of the frame surrounding the pictures corresponds to the color of the related energy curve displayed in Figure 5a.

When the contact area of the drop with the substrate increases (decreases), the number of holes at the drop−substrate interface should increase (decrease). There is a minimum envelope of the curves of Figure 5a that corresponds to the stable configurations for each volume. When two curves intersect, the configurations described by these curves are simultaneously stable. For a given initial condition, changing the volume across such an intersection indicates a change in drop configuration. The liquid has to spread between the holes along certain paths for the drop to reach the next configuration. Along these paths, the drop distorts and reduces its symmetry; this produces an increase in the liquid

surface area and energy. Thus, a drop cannot change its configuration until it can overcome the activation energy barrier separating the configurations, i.e., until it has reached a volume for which the energy barrier disappears. Because of this energy barrier, a drop will not be able to access certain configurations of the minimum envelope of normalized energy.

Figure 6 shows configurations of a drop upon successive volume increments, starting from "in-between 3 holes" (A) and going to "on-top of 3 holes" (D). The transition from (A) to the "in-between 2 holes" (B) occurs at a volume equal to 1. The next transition to "on-top of 1 hole" (C) takes place when the volume of the (B) configuration reaches 1.5. The transition from (C) to "on-top of 2 holes" cannot proceed in the range of volume for which this configuration is the stablest one because the energy required to distort the drop is too large. Thus, the drop switches directly from the (C) to the (D) configuration when its volume reaches 11. Once a drop has enough energy to pass the barrier, the transitions from one symmetric configuration to the next is spontaneous. At the volume for which the transition is allowed, the normalized energy decreases abruptly. Thus, the images of the "transition configurations" do not correspond to minima in the normalized energy, but are snapshots grabbed during the transition. These images are shown to clarify the path taken by the drop to change from one configuration to the next. The series of pictures of Figure 6 show that, when changing between these configurations, the entire drop undergoes displacement relative to the substrate.

In summary, when a drop increases its volume, it undergoes static states and transformations. The static state is where the drop does not change position and maintains an almost constant contact area while the macroscopic contact angle increases (see Figure 3, panels a and b). The transformation occurs when the volume is large enough for the drop to switch to the next lower energy configuration by spontaneously expanding its triple line. Because of the sequential occurrence of static states and transformations on advancing, the triple line successively sticks and slips as the macroscopic contact angle increases gradually and then decreases abruptly. Figure 7 illustrates the normalized energy and the macroscopic contact angle during one stick−slip step on advancing from configuration C to D (depicted in Figure 6).

When the volume of the drop is decreased (i.e., the triple line is forced to recede), there is also an energy penalty associated with configuration changes, and a corresponding stick−slip motion of the triple line on receding. The change from one configuration to the next also proceeds through a distortion of the drop. The distortion of the drop begins before the external triple line merges with the triple lines surrounding the edges of the covered holes. The receding transition occurs at a volume lower than the one at which the normalized energy of the two configurations are equal, as displayed in Figure 7a in the case of the receding transition between configuration D and C. Figure 7b shows the whole hysteresis loop of the macroscopic contact angle between the configurations C and D.

The results of the Evolver calculations are consistent with the experimental results of the companion paper conducted on substrates with holes.[3] Increasing (decreasing) the volume of a sessile drop forces the triple line to advance (recede), as in a liquid bridge experiment where a bridge is compressed (stretched). In the experiments, the nongravity condition is obeyed for the triple line formed on the top substrate. In fact, we observe a stick−slip motion of the triple line and a global motion of the liquid bridge on advancing and receding.[3]

Drops on Posts. As in the case of a surface with circular holes, we have chosen to calculate the shape of drops placed on
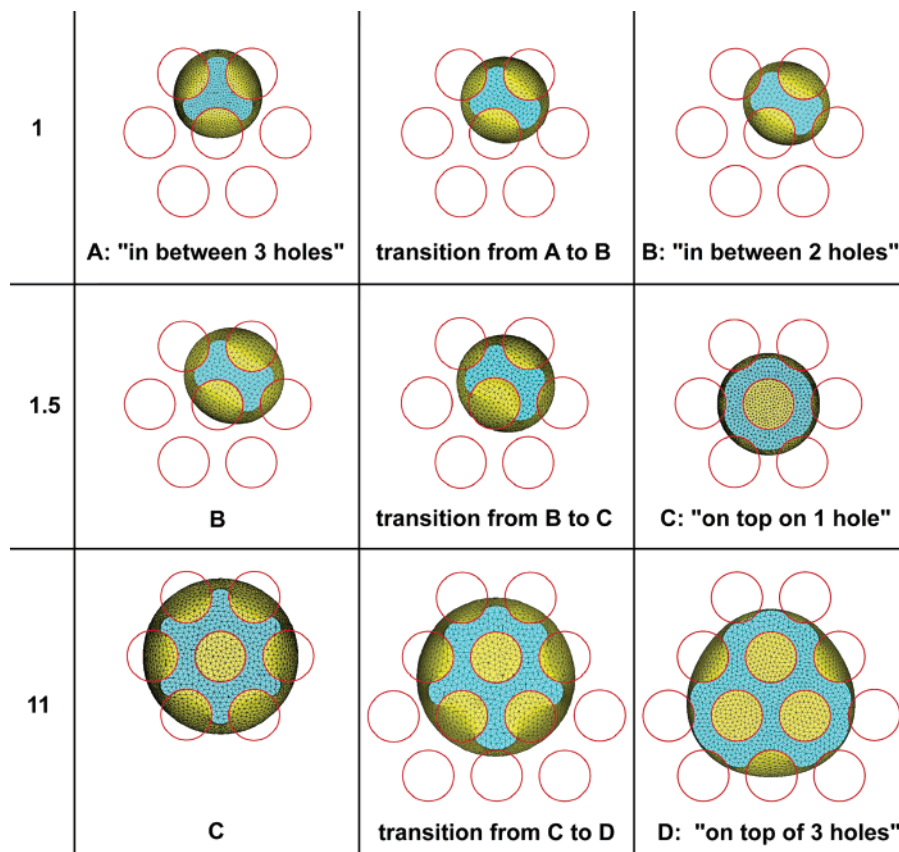
Figure 6. Different stages of the shape of a drop as it advances from "in-between 3 holes" to "on-top of 3 holes". In each row, the drops have the same volume indicated in the left cell.

highly symmetrical positions with respect to the post distribution. Drops covering up to 7 posts have been calculated. Figure 8 shows drops on 1, 2, 3, 4, 5, and 7 posts. The 6-post configuration was always found to be unstable as compared to the 5- and 7-post configurations.

Figure 8a shows the normalized energy of drops on a substrate with circular posts as a function of drop volume. Each of the calculated configurations is displayed in Figure 8b. The color of the frame surrounding the pictures corresponds to the color of the energy curve displayed in Figure 8a. For each configuration the normalized energy is calculated for different volumes ranging about the volume for which the normalized energy is a minimum. As in the case of a surface with holes, there is a minimum envelope of the curves of Figure 8a that corresponds to the stable configurations for each volume.

As was discussed previously, both drop configurations are stable at the intersections of their energy versus volume curves. At constant volume, the drop configuration having the lowest normalized energy is preferred. The mechanisms by which a drop on posts changes its configuration are different from the one discussed for a drop on holes. The main difference arises from the fact that a drop in contact with more than one post has a discontinuous triple line. This point has been stressed by Chen et al.[8] Advancing or receding of the drop is determined by what happens to the segments of triple line contacting the posts at the periphery of the macroscopic solid/liquid interface. Two types of behavior of the triple line are observed. Either it is stuck on the edge of the peripheral posts or it lies on these posts and moves across them when the volume of the liquid is increased

(8) Chen, W.; Fadeev, Y.; Hsieh, M. C.; Oner, D.; Youngblood, J.; MacCarthy, T. J. *Langmuir* **1999**, *15*, 3395.
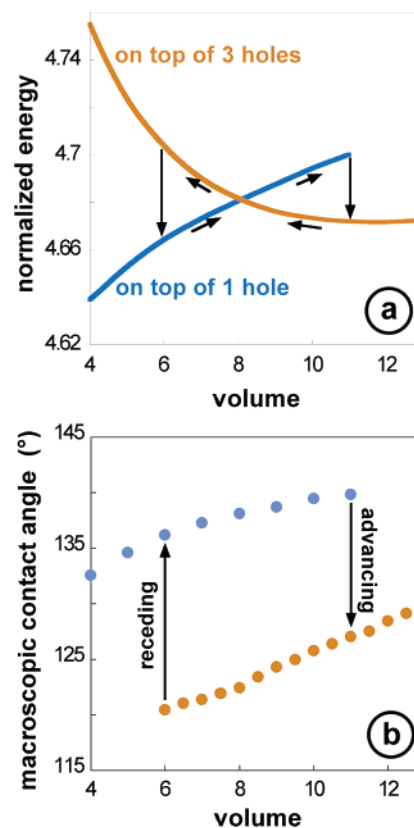
Figure 7. (a) Hysteresis loop on advancing and receding of the normalized energy of drops from "on-top of 1 hole" to "on-top of 3 holes" as function of volume; (b) corresponding hysteresis loop of the macroscopic contact angle of the drop versus volume.
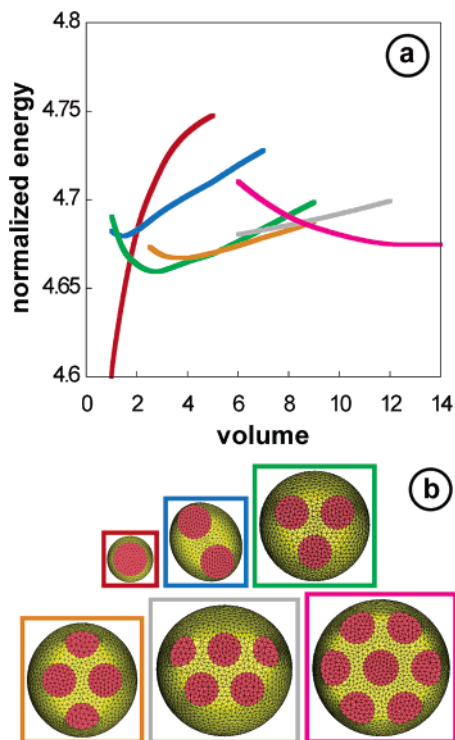
Figure 8. (a) Normalized energy of drops of different configurations on a substrate with posts; (b) bottom views of the different configurations calculated with Evolver.

or decreased. This happens when the local contact angle on the post can adopt the equilibrium value of 110°.

On advancing, a drop cannot jump from one configuration to the next. To advance, the liquid surface must touch another post at the foot of the drop. If the volume of a drop on one post is increased under no-gravity conditions, the drop will remain on that post whatever its volume. Its shape will just be a spherical cap truncated by the circular surface of the post. The larger the volume, the closer the macroscopic contact angle is to 180°. The same type of situation occurs if the drop resides on several posts. During advance, the triple line is attached to the edge of the peripheral posts. This explains the very high advancing angle under no-gravity conditions, as is observed on the top substrate of the liquid bridge experiment.[3] The very high advancing contact angle partly explains the mobility of drops on such surfaces.[8] The liquid surface has to be forced in order to come into contact with new posts in order for the drop triple line to advance. This can be achieved by increasing the pressure in the liquid to change the curvature of the drop. In the liquid bridge experiment, the contact on the top substrate is forced by compressing, whereas on the bottom substrate, the hydrostatic pressure forces the contact with new posts.

On receding, the local contact angle on the post in the Surface Evolver calculations can reach 110°. Thus, the receding contact angle will be smaller than the advancing one and lie closer to the equilibrium angle calculated using the Cassie−Baxter equation

(eq 8). The segments of triple line on the peripheral posts slide backward during receding, and their lengths on the peripheral posts monotononically decreases to zero. When the slipping motion of the line ends, the periphery of the drop is again attached on another set of posts. If there is any sharp detachment from a post, it only changes the mean position of the triple line by the distance between two posts. Thus, the local contact angle can remain at a value of 110° on this new set of posts.

The macroscopic contact angle changes very little on advancing or on receding. This would explain the experimentally observed smooth motion of the triple line on advancing and receding. The superhydrophobic condition is explained by this feature, as there is almost no sticking of the triple line on the surface for both the advancing and receding conditions. The ideal superhydrophobic surface would correspond to a substrate where the surface fraction occupied by the posts is very small, such that the receding angle is close to the advancing one.

Concluding Remarks

The wetting behavior of drops on surfaces with features consisting of holes and posts was studied by numerical methods using Surface Evolver. The energetics of wetting and wetting behavior for droplets on a continuous matrix (smooth surface with holes) have been shown to differ from droplets that wet isolated posts (liquid/vapor surface with posts).

For a given volume of liquid, stable drops sit on more posts than holes. This is because, in the case of holes, a drop can reduce its energy by spreading between the holes when its volume increases, without undergoing a change of configuration. In the case of posts, the drop energy is reduced when the liquid contacts new posts; that is, the drop changes configuration.

For a constant area fraction of wetted surface, the motion of a drop on posts is much easier than on a surface with discontinuous holes because the maximum contact angle hysteresis is nearly constant. This explains, in part, the phenomenon of superhydrophobicity. On surfaces where the triple line is continuous, droplet advancing and receding proceeds by a stick−slip motion of the triple line and wetting hysteresis shows significant scatter. Our calculations show that the drop can be strongly pinned by the edges of the holes.

When the triple line of a drop moves spontaneously, the whole drop moves as well because there is no center of symmetry of the surface features for any value of drop volume. The direction of motion depends on the location of surface features. When the distribution of substrate features contains symmetry, as in this case, there are equivalent displacement directions. Thus, the center of gravity of a drop on a heterogeneous substrate is not fixed and can follow a variety of possible paths as a result of volume increase or decrease.

LA053146Q